

Emergence of superconducting textures in two dimensions

Andreas Glatz,¹ Igor Aranson,¹ Valerii Vinokur,¹ Nikolay Chhtchelkatchev,^{2,3} and Tatyana Baturina⁴

¹*Materials Science Division, Argonne National Laboratory, Argonne, Illinois 60439, USA*

²*L.D. Landau Institute for Theoretical Physics, Russian Academy of Sciences, 117940 Moscow, Russia*

³*Department of Theoretical Physics, Moscow Institute of Physics and Technology, 141700 Moscow, Russia*

⁴*Institute of Semiconductor Physics, 13 Lavrentjev Ave., Novosibirsk, 630090 Russia*

(Dated: May 28, 2018)

Self-organized regular patterns are ubiquitous in nature, and one of their most celebrated manifestations is the Abrikosov vortex lattice¹: under an applied magnetic field, the homogeneous superconductivity becomes unstable and cast itself into a regular texture of the “normal” filaments, called Abrikosov vortices, immersed into a superconducting matrix. Its prediction and the experimental discovery became a breakthrough in our understanding of superconductivity and founded a new direction in physics. Here we show that the interplay between the superconducting order parameter and elastic fields^{2,3,4,5,6}, which are intimately connected to the very existence of the superconductivity itself⁷, can result in a novel superconducting state dual to the Abrikosov state: a regular texture of superconducting islands. The fact that both patterns emerge within the framework of the Ginzburg-Landau description of superconductivity⁸ indicates that the formation of regular structures may be a generic feature of any phase transition. Emergence of superconducting island arrays is not specific to the effect of the elastic forces, but can be caused by any inherent mechanism generating long-range non-local interactions in the Ginzburg-Landau functional, for example, by the Coulomb forces. In particular, our findings suggest the formation of a superconducting island textures as a scenario for a superconductor-to-insulator transition in thin films.

Sixty years ago the volume change accompanying the transition of a superconductor from the normal to the superconducting state was first observed². This discovery – followed by finding the dependence of the superconducting critical temperature, T_c , on the isotopic mass^{9,10} and the change in elastic constants at the transition into the superconducting state^{3,4,5} – geared the line of research crowned eventually by the triumph of the Bardeen-Cooper-Schrieffer (BCS) microscopic theory of superconductivity, which demonstrated an intimate connection between superconductivity and elastic properties of the material⁶. According to the BCS theory, T_c is related to elasticity via⁷

$$k_B T_c = 1.13 \hbar \omega_D \exp \left(-\frac{1}{\nu_0 V} \right), \quad (1)$$

where ω_D is the Debye frequency, ν_0 is the density of states at the Fermi level, and V is the effective interaction strength between electrons mediated by electron-phonon coupling. All three parameters, ω_D , ν_0 , and V in (1) depend on pressure and comprise several microscopic effects including both the changes in the electron and phonon spectrum, as well as structural transformations. The link between elastic properties and superconductivity has been illustrated by numerous experiments revealing the influence of an external pressure on T_c (see refs 11 and 12 for extensive reviews).

Mechanical stresses, which affect superconductivity, are inherent to thin films attached to rigid substrates¹³ (Fig. 1). Indeed, enforcing on the film its own lattice spacing, the substrate impels *internal* strains in the film. On top of that, the rigid coupling between the film and the substrate can give rise to a peculiar scenario of the superconducting transition itself. Upon cooling the film,

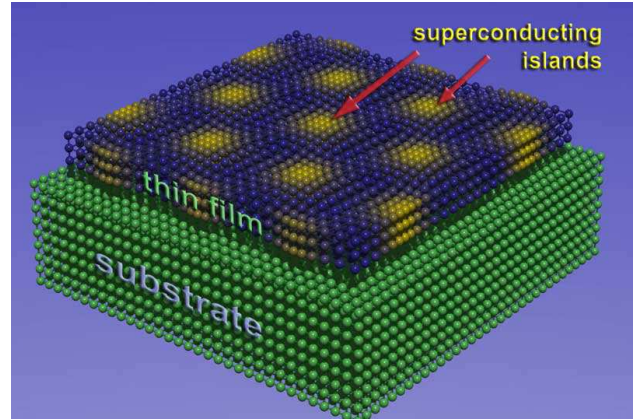


FIG. 1: The system. A sketch of a “soft” superconducting film deposited on a rigid substrate. Mechanical stresses induced by the substrate on the film due to mismatch between the lattice constants of the film and of the substrate, give rise to inhomogeneous superconducting state which emerges in a form of a regular array of separated superconducting islands.

the superconductivity nucleates first in the regions where T_c is elevated by fluctuations. Accordingly, mechanical properties, and, in particular, the lattice spacing in these regions should have changed. The rigid substrate, however, obstructs expansions (contractions) of the film associated with the local onset of superconductivity. As a result, additional local stresses emerge, which, in their turn, promote further growth (and the appearance of new) superconducting nuclei. The role of the substrate is thus twofold: first, it exerts elastic forces in regions where superconducting droplets appear first and, second, the substrate mediates the elastic coupling between re-

mote parts of the film, effectively transforming local distortions into long-range elastic coupling. Appearing and evolving initial superconducting nuclei induce additional elastic distortions. As a result of this positive feedback between the superconducting order parameter and mechanical stress, a spatial instability of the superconducting state develops forming eventually a periodic pattern of superconducting islands (see Fig. 1).

Our starting point is the time-dependent Ginzburg-Landau (TDGL) equation^{8,14,15} combined with elastic stress balance equations (see Methods). This model offers a comprehensive description of formation and temporal evolution of the superconducting nuclei towards the final equilibrium configuration of the order parameter. We choose a random initial configuration for the order parameter which mimics the random distribution of the superconducting nuclei expected to form in a homogeneously disordered film upon cooling it down to T_c . However, the final equilibrium island pattern does not depend on the particular choice of the initial configuration. The advantage of this approach is that all the richness and complexity of the microscopic elasticity-superconductivity interrelations is accounted for by the phenomenological coupling constant $U_0 = 3\alpha_L K(\partial T_c/\partial p)$, where p is the pressure, K is the bulk elastic modulus, and $\alpha_L = (1/L)(\partial L/\partial T)$ is the linear expansion parameter (with L being the linear dimension of the film). These quantities can be inferred from experiments and contain all the information about the electronic degrees of freedom and the lattice excitation spectrum¹⁶.

In the absence of elastic interactions due to connection to a substrate, one has the standard equilibrium solution of the conventional TDGL equation: a spatially uniform order parameter $\psi = \psi_0$ describing the homogeneous superconducting state at $T < T_c$, and $\psi = 0$ at $T > T_c$. The non-local elastic interaction, $U(\mathbf{r} - \mathbf{r}')$, coupling the values of the superconducting order parameter at different points \mathbf{r} and \mathbf{r}' of the film [see Eq. (3) of Methods] distorts ψ_0 and can give rise to an instability of the uniform solution resulting in the formation of a regular island texture for certain values of the elastic parameters. To investigate this process we solve the coupled TDGL and elasticity equations by numerical integration using a quasi-spectral technique. Figure 2 displays a sequence of snapshots for the temporal development of the spatial structure of the amplitude of the order parameter. The time is measured in the units of the Ginzburg-Landau time τ_{GL} , with $\tau_{GL} = \pi\hbar/[8k_B(T_c - T)]$. Starting from the random order parameter configuration, the system evolves through three clearly distinguishable major stages: (i) initial amplification of small fluctuations and emergence of an amorphous structure of islands; (ii) appearance of a polycrystalline configuration of well separated superconducting islands; and (iii) slow relaxation of polycrystalline structure to a regular island lattice. The evolution of the modulus of the order parameter is quantified by the correlation function $\mathcal{C}(t) = \mathcal{N}^{-1} \sum_k |\psi_k|^2$,

where ψ_k denote the Fourier components of the order parameter, and the normalization factor \mathcal{N} is chosen such that $\mathcal{C} = 1$ when the island texture is fully periodic.

The first stage is relatively fast: establishing of an amorphous island pattern takes only about $10\tau_{GL}$, while achieving a polycrystalline structure requires a 10 times longer period. In this intermediate time scale $\mathcal{C}(t)$ evolves logarithmically towards the polycrystalline state. In the final stage, for $t > t_p$, see Fig. 2, where the island polycrystal relaxes towards the regular lattice, the correlation function of the modulus of the order parameter ceases to be an indicative characteristic quantity. At longest time-scales it is rather the temporal development of the spatial distribution of the *phase* of the order parameter that characterizes the evolution of the system. For the chosen material constants the final state is a superconducting state with the uniform phase distribution corresponding to a long-ranged phase coherence. Figure 3 shows that the macroscopic phase-coherent state (which appears as a uniformly colored frame) is achieved via the motion and recombination of vortex-antivortex pairs which are initially present *en mass* in the system due to coalescence of the independent superconducting nuclei in the first stage of the order parameter evolution. The vortex-antivortex pairs are clearly displayed by the “phase-cut” lines that appear as sharp color jumps from black to white. In the same time interval one distinguishes a well pronounced hexagon substructure which shows that different islands have different phases. The global phase coherence and therefore the superconducting state get established by the time of order $10^3\tau_{GL}$, which is by an order of magnitude longer than the time for establishing a robust distribution of the amplitude of the order parameter.

It is important that, while being a general phenomenon, the formation of an island texture requires the elastic coupling to be strong enough. Namely, the texture appears under the condition that the coupling constant U_0 exceeds some temperature dependent critical value $U_c(T)$. The function $U_c(T)$ is determined by means of linear stability analysis of the TDGL. Writing down the Fourier transform of the elastic interaction term $U(\mathbf{r})$ as $\tilde{U}(q) = U_0\mathcal{K}(q)$, where $\mathcal{K}(q)$ is the scale free elastic kernel in the momentum space and γ is the diffusion coefficient in the Ginzburg-Landau equation (see Method), one finds that the island state forms if $(U_0\mathcal{K}_M - 1)(1 - T) - \gamma q_M^2/9.38 \geq 0$, where \mathcal{K}_M is the maximum value of $\mathcal{K}(q)$ at $q = q_M$. This gives $U_c(T) = \mathcal{K}_M^{-1} + (\gamma q_M^2/9.38\mathcal{K}_M)(1 - T/T_c)^{-1}$. The lower bound for the coupling constant at which the homogeneous state becomes unstable and the island texture can appear is $U_c = (\gamma q_M^2/9.38 + 1)/\mathcal{K}_M$. The left panel of the Figure 4 shows the phase diagram in the reduced T/T_c - U_0/U_c coordinates for the chosen system parameters which are given in the Methods. The right panel of Fig. 4 shows the behavior of the amplitude of the order parameter $|\Delta|$ at the isotherm $T = 0.8T_c$ as function of the coupling constant U_0 . The protocol for finding this dependence is as follows: We start with a coupling con-

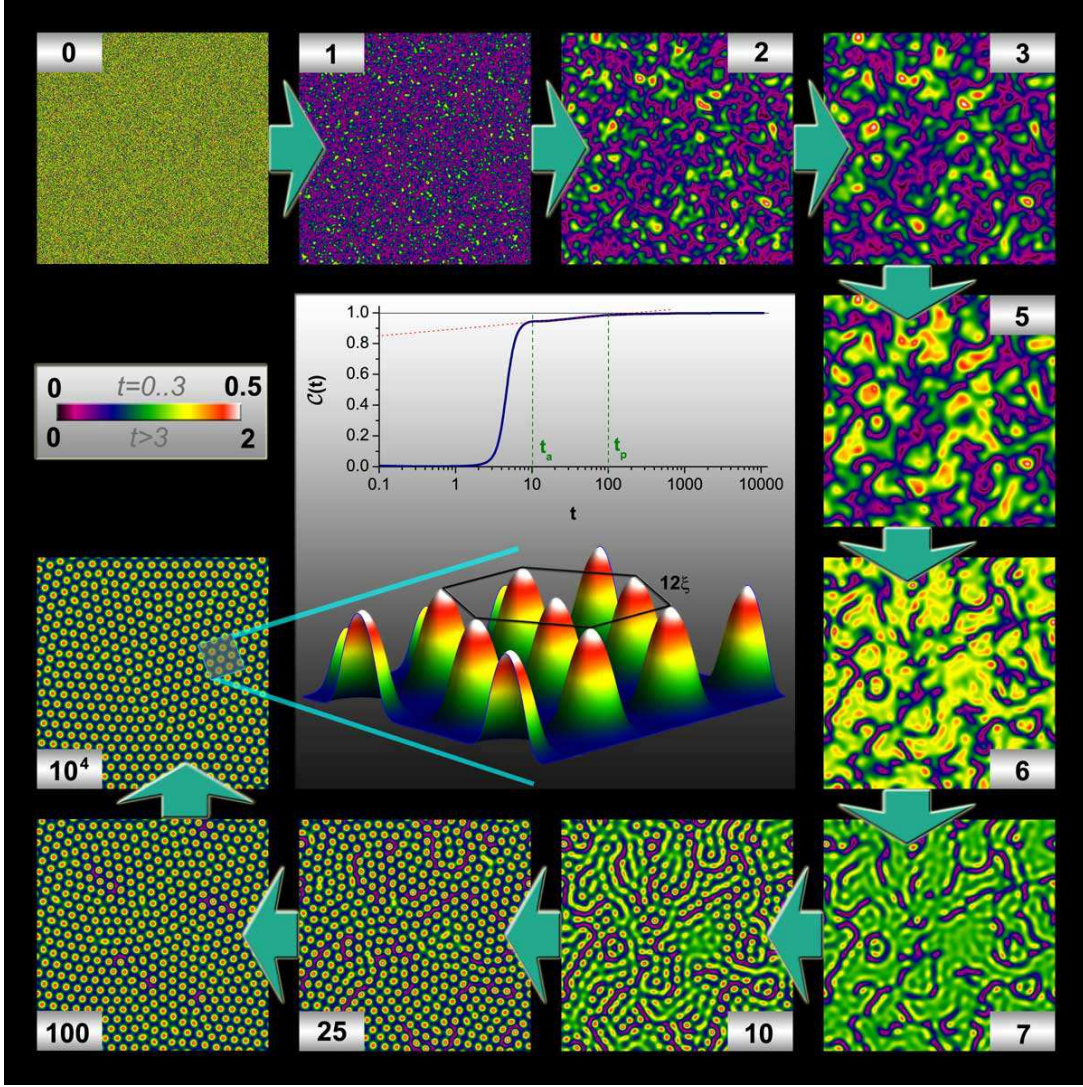


FIG. 2: **Formation of the island texture.** The framing sequence of snapshots shows the temporal evolution of the spatial distribution of the amplitude of the superconducting order parameter. The time is measured in units of the Ginzburg-Landau time, which for temperature $T = 0.8T_c$ can be estimated as $\tau_{GL} \simeq 10^{-11}$ seconds for $T_c \approx 1\text{K}$. The first frame at time $t = 0$ shows an initial random configuration of the order parameter. One can distinguish three stages of the evolution: (i) emergence of an amorphous structure of islands (for $t < t_a \sim 10$); (ii) formation of a polycrystalline islands texture (for $t_a < t < t_p \sim 100$) and (iii) relaxation to a long-range ordered island lattice (for $t > 10^4$). The color bar for the amplitude of the order parameter is presented beneath the initial frame (note the change of the scale for $t > 3$). The upper part of the central panel shows the time evolution of the normalized order parameter correlation function, $\mathcal{C}(t) = \mathcal{N}^{-1} \sum_k |\psi_k|^2$, vs t on a logarithmic scale (ψ_k denote the Fourier components of the order parameter and the normalization factor \mathcal{N} is chosen such that $\mathcal{C} = 1$ when the island texture is fully periodic). At intermediate times between t_a and t_p the correlation function shows transient logarithmic behavior (highlighted by the straight line) and exhibits for $t > t_p$ a slow convergence to unity. The lower part shows a perspective view of the height profile of the amplitude of the order parameter corresponding to a small region of the perfect lattice appearing at the final stage of solution of the TDGL equation. The simulations were done with the coupling constant of $U_0 = 2.23U_c$ and the thickness of the film of 0.8ξ , where ξ is the superconducting coherence length at zero temperature. Defining an “island” as an area within which the amplitude of the order parameter exceeds half of its maximal value, we find their size to be about 2.5ξ and the distance between the centers of the islands to be 12ξ .

stant $U_0 < U_c$ and an initial random distribution of the order parameter, and let the system evolve until a stationary distribution of Δ is achieved. After that U_0 is increased and the system evolves again until a new stationary state is achieved (adiabatic increase), and so forth.

Upon crossing the phase boundary a bifurcation in the $|\Delta(U_0)|$ -dependence corresponding to the islands formation occurs and a *finite* difference between the maximal and minimal values of the amplitude of the order parameter appears. In other words $|\Delta(U_0)|$ shows finite jumps

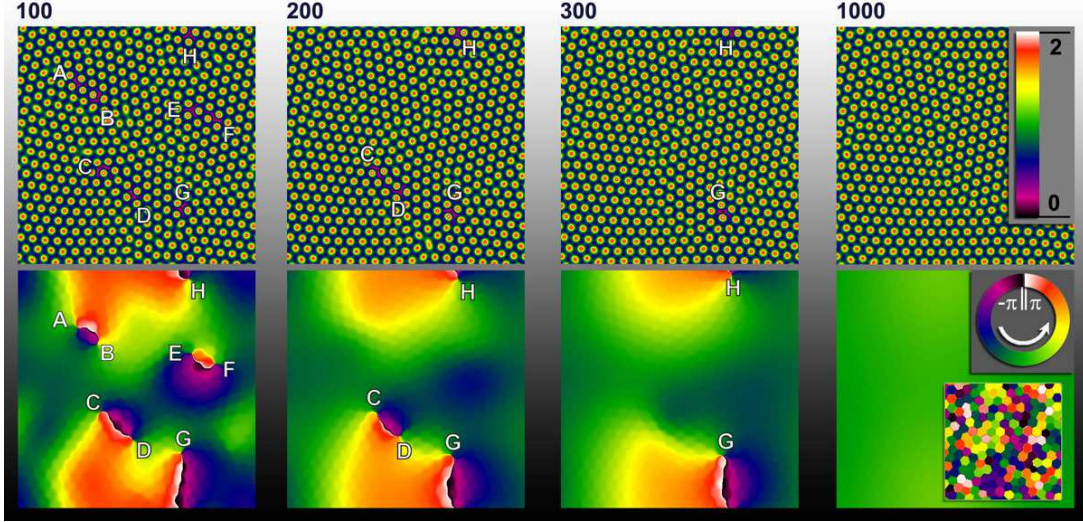


FIG. 3: **Temporal evolution of the amplitude and phase of the order parameter.** Four sequential snapshots of the amplitude and phase of the order parameter taken at times 100, 200, 300, and 1000 measured in units of τ_{GL} are presented (the same values of the system parameters as in Figure 2 were used). The first three frames correspond to nonequilibrium states characterized by an inhomogeneous phase distribution; in this stage the formation of a regular texture of the order parameter amplitude goes along with the recombination of vortex-antivortex pairs. The first frame displays four sets of vortex-antivortex pairs with the endpoints **A-B**, **C-D**, **E-F**, and **G-H**. In the corresponding phase frames these endpoints confine the line of 2π phase jumps visible as sharp color change from white to black (the periodic boundary conditions were used, such that the line **G-H** goes over the upper- and lower edges of the frame). The phase cut lines **A-B** and **E-F** disappear at $t = 200$, and at $t = 300$ only the **G-H** line remains. In the nonequilibrium states, the hexagon-like structure of the phase distribution reflecting that on the way to equilibrium the phase at the islands are different is clearly distinguishable (each hexagon represents the phase of an island). At $t = 1000$ the phase becomes homogeneous across the sample and a global phase-coherent superconducting state establishes. However, for a different set of parameters the phase equilibration might be very slow or even stopped in the presence of impurities or dissipation, resulting in a random pattern of phases for each island, shown in the inset of the last phase-frame.

to the $|\Delta_{\min}(U_0)|$ and $|\Delta_{\max}(U_0)|$ branches at some U_0 appreciably beyond the phase boundary. On the descending part of the cycle, $|\Delta_{\min}(U_0)|$ and $|\Delta_{\max}(U_0)|$ merge at smaller value of U_0 closer to the phase boundary, i.e. at smaller U_0 . The change of U_0 is indicated by the vertical arrow in the left panel of Fig. 4. Shown in the right panel inset is the hysteretic behavior of the order parameter corresponding to sweeping the temperature across the phase transition line. The protocol is nearly the same as for the coupling constant variation scheme; the temperature is first decreased from $T = T_c$ down to $T = 0.8T_c$ and then increased back at the fixed coupling constant $U_0 = 2.6U_c$. The temperature sweeping is indicated by the horizontal arrow in the left panel of Fig. 4. Note that the island structure persists even as the system is heated above T_c ; this is the manifestation of the positive feedback between the superconductivity and elasticity in this films bonded to the substrate giving rise to a local increase in superconducting transition temperature within the islands. The observed hysteretic behaviors indicate that the transition between the homogeneous superconducting and the island texture states is of the first order.

The pattern formation and, in particular, the spontaneous emergence of electronic nanometer-scale structures, due to the existence of competing states is ubiqui-

tous in nature and is found in a wealth of complex systems and physical phenomena ranging from magnetism, superconductivity and superfluidity to liquid crystals and biological dynamics^{15,17}. The Ginzburg-Landau equation, one of the most universal models in theoretical physics, offers an adequate quantitative description of the pattern formation. Here we have revealed the instability and emergence of an electronic textures, due to coupling of the superconducting order parameter with elastic stress fields, generating a non-local term in the Ginzburg-Landau functional. It is noteworthy that the general form of the nonlocality in the Ginzburg-Landau equation, induced by the interplay between the local nonlinearity and the nonlocal couplings, is universal and can result from various physical mechanisms. In particular, while the results presented here are stable with respect to weak disorder, we expect that the interplay of strong disorder with Coulomb interactions will give an essential contribution to the nonlocal coupling in the Ginzburg-Landau functional. Note, in this connection the interesting discussion of the effects of disorder leading to a spatially inhomogeneous distribution of the order parameter^{18,19,20,21,22}. We thus conclude that a consistent consideration of the superconductivity in thin films has to include the effects of the interplay between strong

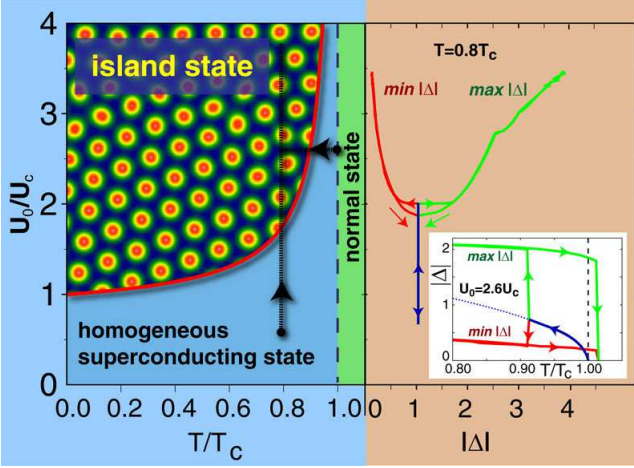


FIG. 4: **Phase diagram and hysteretic onset of the island texture.** The left panel shows the phases in the temperature T - coupling constant, U_0 , plane. Above T_c the film is in the normal state, whereas below T_c the film can be either a homogeneous superconductor or a textured superconductor consisting of isolated islands. The phase boundary is determined by the stability condition of the TGLE (see text). The right panel shows the amplitude of the order parameter Δ as function of the coupling constant U_0 . The onset of the island texture (crossing the phase boundary) is marked by the bifurcation point where Δ_{\max} and Δ_{\min} start to diverge. The observed hysteretic behavior – the island structure forms, upon adiabatically increasing the coupling, at larger value of U_0 than the reverse transition, upon decreasing U_0 , to the spatially homogeneous order parameter state – indicates that the formation of the island texture occurs via a first order transition. The path of change of U_0 is indicated by the vertical arrow in the left panel. The inset in the right panel shows the hysteretic effect corresponding sweeping temperature at fixed $U_0 = 2.6U_c$, first, from T_c down to $0.8T_c$, and then heating up (the process shown by the horizontal dotted line in the left panel). It is noteworthy that the island structure persists even upon heating the system above T_c of the film material, due to the increased local T_c within the islands. The dotted line indicates the usual $\sqrt{1 - T/T_c}$ behavior of the order parameter without elastic interactions.

disorder with Coulomb interactions and elasticity.

The observed island texture is an array of granules of a “good” superconductor immersed into a sea of a “bad” one with much smaller amplitude of the order parameter and is equivalent to an array of small superconducting droplets connected via weak links, i.e., a Josephson junction array (JJA). In our simulations, where thermal and quantum fluctuations are absent, the Josephson coupling, however weak, eventually establishes a global phase coherence and thus global superconductivity. The fluctuations, dissipation, and disorder can break down this phase uniformity: the intermediate stages of phase distributions of our simulations represent the final states of the “real world” systems. Thus the possible eventual configuration of the order parameter phase (see the “Gaudimosaic” phase distribution in the inset of the last phase-

frame of the Fig. 3) can correspond even the insulating state. This is in accord with the general result that JJAs turn insulators if the Josephson coupling between the superconducting islands becomes sufficiently weak²³. Thus our finding that the transition into a superconducting state in two dimensional superconductors elastically tied to a substrate can occur via the formation of nanoscale superconducting island pattern offers a possible scenario for the superconductor-to-insulator transition observed in various thin superconducting films^{24,25,26,27,28,29}. This supports the conjecture^{30,31} that the formation of a regular array of superconducting droplets is an inherent property of the critical region of the superconductor-to-insulator transition.

Acknowledgments

We thank Yuri Galperin and David Hinks for useful discussions. This work was supported by the U.S. Department of Energy Office of Science under the Contract No. DE-AC02-06CH11357, by the Program “Quantum macrophysics” of the Russian Academy of Sciences, and by the Russian Foundation for Basic Research (Grant Nos. 09-02-01205 and 09-0212206).

APPENDIX A: ADDENDUM

1. Ginzburg-Landau equation.

The two-dimensional time-dependent Ginzburg-Landau equation (TGLE) describing the behavior of the film is written, in dimensionless variables as:

$$\partial_t \psi = \alpha \psi - \beta |\psi|^2 \psi + \gamma \nabla^2 \psi - \delta |\psi|^4 \psi, \quad (\text{A1})$$

where $\psi = \psi(\mathbf{r}, t)$ is the complex, dimensionless superconducting order parameter normalized with respect to T_c . We consider the static case where the external fields are absent, thus the electro-magnetic potentials can be absorbed into the order parameter. We include a small sixth order term in the GL free energy to ensure a numerical stability. The coefficient $\alpha = \alpha_\psi(\mathbf{r})$ is a functional of the order parameter and includes the effects of long-range elastic potentials, temperature T , and disorder:

$$\alpha_\psi(\mathbf{r}) = \alpha_0 [T_c(\mathbf{r}) - T] + \int d\mathbf{r}' U(\mathbf{r} - \mathbf{r}') |\psi(\mathbf{r}', t)|^2, \quad (\text{A2})$$

where $T_c(\mathbf{r}) = T_c(1 + \tau(\mathbf{r}))$ describes quenched fluctuations ($\tau(\mathbf{r}) \in [-\lambda; \lambda]$) of T_c and $U(\mathbf{r} - \mathbf{r}')$ is the non-local kernel generated by elasticity interactions. The temperature T is measured in units of superconducting transition temperature T_c , and the unit of the length is the superconducting, zero temperature coherence length ξ .

2. Elastic interaction.

To couple elasticity and superconductivity we utilize the pressure dependence of $T_c(p)$ which is taken in a linearized form as

$$T_c(p = p_0 + \Delta p) = T_c(p_0) + \Delta p \frac{\partial T_c(p_0)}{\partial p}, \quad (\text{A3})$$

where Δp is the change in the internal pressure induced by elastic forces. The latter is derived from the condition of the continuity of the deformation fields $\mathbf{u}^{(s,p)}$ and the stress balance at the film-substrate interface (the $z = 0$ plane),

$$\sigma_{iz}^{(s)}(0, 0, 0) = \sigma_{iz}^{(p)}(0, 0, 0) \quad \text{for} \quad i = x, y, z,$$

and

$$u_i^{(s)}(0, 0, 0) = u_i^{(p)}(0, 0, 0) \quad \text{for} \quad i = x, y, z,$$

and at the film-vacuum ($z = d$, d is the thickness of the film) interface:

$$\sigma_{iz}^{(s)}(0, 0, d) = 0 \quad \text{for} \quad i = x, y, z. \quad (\text{A4})$$

The superscripts (s) and (p) refer to the film and to the substrate respectively.

These nine coupled equations are solved using a plain-wave Ansatz, yielding the exact expressions for the deformation fields which, in their turn, are used for calculating the internal pressure of the film. The Fourier transform of the pressure in the film then reads:

$$p^{(s)}(\mathbf{q}) = \frac{1}{3d} \int_0^d dz \left(\partial_x u_x^{(s)} + \partial_y u_y^{(s)} + \partial_z u_z^{(s)} \right). \quad (\text{A5})$$

Using this expression together with the relation $\Delta p = -K\Delta V/V$ in Eq. (A3) one finds the parameter α of the TDGL in the form given in (B7). We define the interaction potential $U(r)$ through its Fourier transform $U_0 \mathcal{K}(q)$, where $U_0 = 3K\Delta\alpha_L[\partial T_c(p_0)/\partial p]$ and $\mathcal{K}(q)$ is the scale free part of $p^{(s)}(\mathbf{q})/|\psi_q|^2$ [note, that $p^{(s)}(\mathbf{q}) \propto |\psi_q|^2$]. Here K is the bulk modulus, the linear thermal expansivity of the film is $\Delta\alpha_L$, and the relative volume change due to the change in pressure Δp is $\Delta V/V$.

3. Numerical simulation.

The TGLE (B9) is solved on a fine discrete grid by the numerical integration in real- and Fourier spaces (*quasi-spectral split-step method*), taking into account the full non-local elastic potential. We use periodic boundary conditions and $N = 512^2$ grid points for a system of the size $L^2 = (200\xi)^2$. The temperature is chosen as $T = 0.8T_c$ and the coupling constant of $U_0/U_c = 2.23$ (in Figs. 2 and 3) for a film of thickness $d = 0.8\xi$. The used GL parameters are $\alpha_0 = 4.37$, $\beta = 1/2$, $\gamma = 0.01$, and $\delta = 0.1$. The parameters of the elastic kernel are $\mu^{(s)} = 0.5$, $\mu^{(p)} = 5.0$ (shear moduli) and $\nu^{(s,p)}/(1 - 2\nu^{(s,p)}) = 1.6$ (modified Poisson numbers) – see supplementary materials for details.

APPENDIX B: SUPPLEMENTARY CALCULATIONS

1. Construction of the elastic interaction potential U

Here we derive $U(\mathbf{r})$ for the problem of a thin superconducting elastic film coupled to a rigid substrate with different elastic properties and lattice mismatch. In the following, we use the superscripts (s) for all quantities related to the film, and (p) for the substrate. Both materials are described by the three dimensional displacement fields $\mathbf{u}^{(s)}/\mathbf{u}^{(p)}$. We start our consideration using a plain wave Ansatz for these fields:

$$\begin{aligned} u_x^{(s)} &= e^{iq_x x + iq_y y} \left(e^{q_z z} A_{1,x} + A_{2,x} e^{-q_z z} + u_{0,x}^{(s)} \right) \\ u_y^{(s)} &= e^{iq_x x + iq_y y} \left(e^{q_z z} A_{1,y} + A_{2,y} e^{-q_z z} + u_{0,y}^{(s)} \right) \\ u_z^{(s)} &= e^{iq_x x + iq_y y} \left(e^{q_z z} A_{1,z} + A_{2,z} e^{-q_z z} \right) \\ u_x^{(p)} &= C_x e^{q_z z + iq_x x + iq_y y} \\ u_y^{(p)} &= C_y e^{q_z z + iq_x x + iq_y y} \\ u_z^{(p)} &= C_z e^{q_z z + iq_x x + iq_y y}, \end{aligned}$$

where the misfit strain on the film is captured by the real exponential terms of the film in z -direction. $u_{0,x}^{(s)}$ and $u_{0,y}^{(s)}$ are special solutions of the two-dimensional problem due to superconductivity, which we will discuss later. In order to determine the nine free parameters C_i , $A_{1,i}$, and $A_{2,i}$ we need nine equations. First, we consider the interface film-vacuum at $z = d$, where d is the thickness of the film. The stress boundary condition for a flat surface demands: $\sigma_{xz} = \sigma_{yz} = \sigma_{zz} = 0$. So, for the film we get from Hooke's law

$$\begin{aligned} \sigma_{xz}^{(s)} &= \mu^{(s)} \left(\partial_z u_x^{(s)} + (1 - 2\sigma_0) \partial_x u_z^{(s)} \right) \\ \sigma_{yz}^{(s)} &= \mu^{(s)} \left(\partial_z u_y^{(s)} + (1 - 2\sigma_0) \partial_y u_z^{(s)} \right) \\ \sigma_{zz}^{(s)} &= 2\mu^{(s)} \left[\left(1 + \nu^{(s)} \right) \partial_z u_z^{(s)} + \nu^{(s)} \left(\partial_x u_x^{(s)} + \partial_y u_y^{(s)} \right) \right], \end{aligned}$$

where the effect of a lattice mismatch of both materials is captured by the σ_0 -term. In general, the lattice constants of both materials are different, i.e., the misfit parameter $\eta = (a^{(s)} - a^{(p)})/a^{(p)}$ is non-zero, where $a^{(s)}$ and $a^{(p)}$ are the lattice constants of the film and substrate, respectively. This lattice mismatch leads to a compression of the film-lattice at the interface, such that the lattice spacings match there. We note, that this description not only applies to crystalline structures but also for amorphous materials, where the "lattice" constants are averaged quantities.

The coefficients $\mu^{(s)}$ and $\nu^{(s)}$ are the shear modulus and the modified Poisson number of the film [$\nu^{(s)} = \tilde{\nu}^{(s)}/(1 - 2\tilde{\nu}^{(s)})$, where $\tilde{\nu}^{(s)}$ is the Poisson number]. In the following we use the fact, that all interface equations are independent of the x and y coordinate and set $x = y = 0$.

Therefore, the first three of the nine equations are

$$\sigma_{iz}^{(s)}(0, 0, d) = 0 \text{ for } i = x, y, z. \quad (\text{B1})$$

Next, we consider the interface between film-substrate at $z = 0$, for which we also need the expressions for the stress tensor elements

$$\begin{aligned} \sigma_{xz}^{(p)} &= \mu^{(p)} \left(\partial_z u_x^{(p)} + \partial_x u_z^{(p)} \right) \\ \sigma_{yz}^{(p)} &= \mu^{(p)} \left(\partial_z u_y^{(p)} + \partial_y u_z^{(p)} \right) \\ \sigma_{zz}^{(p)} &= 2\mu^{(p)} \left[\left(1 + \nu^{(p)} \right) \partial_z u_z^{(p)} + \nu^{(p)} \left(\partial_x u_x^{(p)} + \partial_y u_y^{(p)} \right) \right]. \end{aligned}$$

At this interface we need to fulfill six more conditions, where three of them are resulting from the stress balance

$$\sigma_{iz}^{(s)}(0, 0, 0) = \sigma_{iz}^{(p)}(0, 0, 0) \text{ for } i = x, y, z,$$

and the last three equations are the continuity equations for the displacement fields

$$u_i^{(s)}(0, 0, 0) = u_i^{(p)}(0, 0, 0) \text{ for } i = x, y, z.$$

These nine equations can now be solved in order obtain the free parameters of our Ansatz.

The two special solutions for $u^{(s)}$ in x- and y-direction, $u_{0,i}^{(s)}$, already used in the Ansatz for the deformation fields of the film are obtained through solution of the extended stress-strain balance

$$\beta^{(s)} \Delta \mathbf{u}^{(s)} + \nabla(\nabla \mathbf{u}^{(s)}) = \gamma^{(s)} \nabla |\psi(\mathbf{r})|^2, \quad (\text{B2})$$

which takes into account that the systems energy is the sum of the superconducting energy and the mechanical deformation energy. This relation introduces two phenomenological parameters: $\gamma^{(s)}$ and $\beta^{(s)}$ which together define the coupling constant of the elastic interaction and superconductivity which is determined explicitly below. Eq. (B2) can be solved and gives

$$u_{0,i}^{(s)} = -i\gamma_s \frac{f(q)q_i}{(1 + \beta_s)\mathbf{q}^2}, \quad (\text{B3})$$

for $i = x, y$.

Using the solutions for all coefficients we find the internal pressure of the film

$$p^{(s)}(q_x, q_y, q_z) = \frac{1}{3d} \int_0^d dz \left(\partial_x u_x^{(s)} + \partial_y u_y^{(s)} + \partial_z u_z^{(s)} \right). \quad (\text{B4})$$

This expression simplifies to $p^{(s)}(q_z)$ if we use the homogeneous parametrization $q_x = q_z \cos(\theta)$, $q_y = q_z \sin(\theta)$. Due to the special solution for $u^{(s)}$ the pressure $p^{(s)}(q)$ is proportional to $|\psi_q|^2$, where ψ_q are the Fourier components of the order parameter.

Now, we need to consider the connection of elasticity and superconductivity. For that, we first expand T_c in changes of (internal) pressure:

$$T_c(p = p_0 + \Delta p) = T_c(p_0) + \Delta p \frac{\partial T_c(p_0)}{\partial p}. \quad (\text{B5})$$

The pressure change Δp is related to a volume change ΔV as $K = -V\partial p/\partial V$, where K is the bulk modulus. Therefore we can write

$$\Delta p = -K \frac{\Delta V}{V} = -3K \frac{\Delta L}{L} \propto -3K\alpha_L, \quad (\text{B6})$$

where $\Delta L/L$ is the relative length change of the system and α_L the linear thermal expansivity of the film.

Using the above result in the pressure-expanded critical temperature, the parameter α in the TGLE obtains thus the non-local form shown in the **Methods Summary** section:

$$\alpha_\psi(\mathbf{r}) = \alpha_0 [T_c(\mathbf{r}) - T] + \int d\mathbf{r}' U(\mathbf{r} - \mathbf{r}') |\psi(\mathbf{r}', t)|^2, \quad (\text{B7})$$

where $T_c(\mathbf{r})$ includes also spatial variations of T_c due to weak disorder.

If we define the scale free elastic kernel

$$\mathcal{K}(q) = \frac{(1 + \beta^{(s)})}{\gamma^{(s)}} \frac{p^{(s)}(q)}{|\psi(\mathbf{r})|^2}, \quad (\text{B8})$$

where the explicit form of the elastic kernel is quite involved and given in section B3. Finally, we write the Fourier transform of $U(\mathbf{r})$ as $U_0 \mathcal{K}(q)$, where $U_0 = 3K\Delta\alpha_L[\partial T_c(p_0)/\partial p]$

2. Numerical realization

The TGLE equation

$$\partial_t \psi = \alpha \psi - \beta |\psi|^2 \psi + \gamma \nabla^2 \psi - \delta |\psi|^4 \psi, \quad (\text{B9})$$

is solved by a quasi-spectral split step method for periodic boundary conditions on a two-dimensional square grid with grid size of N^2 for a system size L^2 . *Split step* means, that for each time step the equation is solved partially in real space and partially in Fourier space (the diffusion part)¹⁵. In the first step we calculate

$$\psi_{ij}(t + \Delta t) = e^{\Delta t(\alpha - \beta |\psi_{ij}|^2)} |\psi_{ij}(t)|^2, \quad (\text{B10})$$

where the non-local part of α is calculated by Fast-Fourier-Transformation (FFT) upfront.

Then, in the second step, we first Fourier transform $\psi_{ij}(t + \Delta t)$, apply the diffusion kernel, and transform it back. This way we avoid mostly all complications of the diffusion equation¹⁵.

In general the TGLE without long-range potential has only two stable solutions: a homogeneous one and a striped phase. Even if a long-range potential is present, the stability of these two solutions is only destroyed under certain conditions which can be found out by linear stability analysis (see next section). E.g., a Coulomb potential or even screened Coulomb potential cannot create this kind of instability. However, the elastic potential does, if the model parameters are chosen appropriately. Another possible non-local potential which destroys the homogeneous/striped solutions is a box-potential³² $U(\mathbf{r}) = U_0 \Theta(1 - |\mathbf{r}|/a)$.

TABLE I: List of parameters for the elastic model.

d	thickness of the film
$\mu^{(s,p)}$	shear modulus
σ_0	deformation stress
$\nu^{(s,p)}$	modified Poisson number
U_0	potential strength
κ	coupling constant
$\sigma_{ij}^{(s,p)}$	stress tensor
$u_i^{(s,p)}$	displacement fields
$A_{1,i}, A_{2,i}, C_i$	9 free variables for the elastic equations

3. Elastic kernel and simulation parameters

In order to determine whether the elastic long-range interactions lead to an instability of the homogeneous solution ψ_0 of the GL equation, we need to check the linear stability of the equation, by expanding the order parameter around ψ_0 . After this expansion and Fourier transformation, we find that the stability depends on the behavior of the function

$$S(q) = (2U_0\mathcal{K}(q) - 1)(1 - T/T_c) - \gamma q^2/9.38. \quad (\text{B11})$$

We know that $\mathcal{K}(q=0) = 0$ and $\mathcal{K}(q \rightarrow \infty) = 1/3$ and therefore $S(q=0) < 0$ (for $T < T_c$) and $S(q) \rightarrow -\infty$ for

$q \rightarrow \infty$. If $S(q)$ changes its sign at intermediate q the homogeneous solution becomes unstable, see Fig. 5.

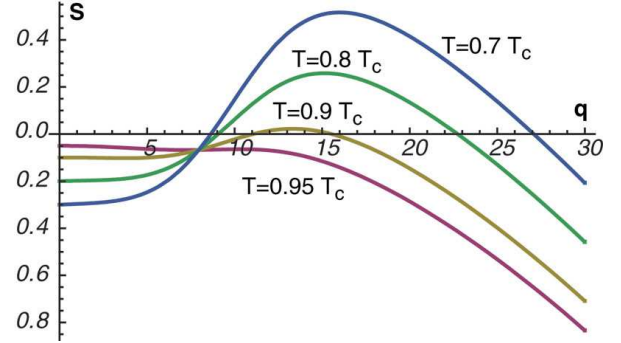


FIG. 5: **Linear stability.** Plot of the stability function $S(q)$ with elastic parameters chosen as described in the text for different temperatures and $U_0 = 2.6U_c$ (cf. inset of Fig. 4).

For completeness we write the scale free elastic kernel \mathcal{K} explicitly, depending only on dimensionless material parameters:

$$\begin{aligned}
\mathcal{K}(q) = & \left\{ \mu_p^2 (1 + 2\nu^{(p)}) \left[d q (1 + e^{4d q}) \vartheta_s - (e^{4d q} - 1) (2\vartheta_s + 1) \right] \right. \\
& + d q \left[e^{4d q} \mu_s \vartheta^{(s)} (2\mu^{(p)} + 2\mu^{(p)} \nu^{(p)} \sigma_0 - \mu^{(s)} \vartheta^{(s)}) \right. \\
& \quad - \mu^{(s)} \vartheta^{(s)} (\mu^{(s)} \vartheta^{(s)} + 2\mu^{(p)} [1 + \nu^{(p)} + \nu^{(s)} - \nu^{(p)} \sigma_0]) \\
& \quad \left. - 2e^{2d q} q (\mu^{(p)^2} [1 + 2\nu^{(p)}] [1 + 2\nu^{(s)} \sigma_0] - \mu^{(s)^2} \vartheta^{(s)^2} - \mu^{(p)} \mu^{(s)} \vartheta^{(s)} (\nu^{(p)} + \nu^{(s)} - 2\nu^{(p)} \sigma_0)) \right] \\
& + \mu^{(s)} (e^{d q} - 1)^2 \left[4\mu^{(s)} \nu^{(s)} (e^{2d q} - 1) \vartheta^{(s)} [\sigma_0 - 1] \right. \\
& \quad + \mu^{(p)} [1 + 2\nu^{(s)} (2 - 2\vartheta^{(s)} - 3\sigma_0) + 2\nu^{(p)} [2\vartheta^{(s)} + 1] [\sigma_0 - 1] - 2e^{d q} (\nu^{(s)} (2\nu^{(p)} [\sigma_0 - 1] + 2\sigma_0 - 3) - 1) \\
& \quad \left. - e^{2d q} q (3\vartheta^{(s)} + 2 + 2\nu^{(p)} [\sigma_0 - 1] (\nu^{(s)} [4\sigma_0 - 2] - 1)) \right] \\
& + 4\mu^{(p)^2} \nu^{(s)} e^{2d q} [1 + 2\nu^{(p)}] [4\sigma_0 - 3] \sinh(d q) \left. \right\} / \\
& \left\{ 3d q \left\{ -\mu^{(s)^2} (e^{2d q} - 1)^2 \vartheta^{(s)^2} \right. \right. \\
& \quad + 2\mu^{(p)} \mu^{(s)} (e^{2d q} - 1) \vartheta^{(s)} (1 + \nu^{(p)} + \nu^{(s)} - \nu^{(p)} \sigma_0 + e^{2d q} [1 + \nu^{(p)} \sigma_0]) \\
& \quad \left. \left. + \mu^{(p)^2} (1 + 2\nu^{(p)}) (e^{4d q} \vartheta^{(s)} + 2\nu^{(s)} [\sigma_0 - 1] - 1 - 2e^{2d q} [1 + 2\nu^{(s)} \sigma_0]) \right\} \right\} \quad (\text{B12})
\end{aligned}$$

with $\vartheta^{(s)} \equiv 2\nu^{(s)} [\sigma_0 - 1] - 1$ and parameters described in table B 3.

For the simulations (cf. evolution of amplitude and phase in Figs. 2 and 3) we used the typical values: $T = 0.8T_c$, $U_0 = 2.2U_c$, $\gamma = 0.01$, $\beta = 0.5$, $d = 0.8\xi_0$,

$\mu^{(s)} = 0.5$, $\mu^{(p)} = 5$ (the substrate is more rigid), $\nu^{(s)} = \nu^{(p)} = 1.6$, $\sigma_0 = 0$ (the lattice mismatch in the normal state is not relevant), $L = 200\xi_0$ (linear dimension of the system), and $N = 512$ (number of discrete grid points per dimension).

¹ Abrikosov, A. A. On the Magnetic Properties of Superconductors of the Second Group. *Soviet Physics JETP* **5**,

- (1957).]
- ² Lasarev, B. G. & Sudovtsov, A. I. On the change of the volume of tin upon superconducting transition in a magnetic field. *Dokl. Akad. Nauk S.S.S.R.* **69**, 345-347 (1949).
 - ³ Landauer, J. K. Elastic Moduli of Tin at the Superconducting Transition. *Phys. Rev.* **96**, 296-301 (1954).
 - ⁴ Olsen, J. L. Change of Elastic Constants in a Superconductor. *Nature* **175**, 37- (1955).
 - ⁵ Grassman, P. & Olsen, J. L. Change in the shear modulus of tin at the transition from the normal conducting to the superconducting state. *Helv. Phys. Acta* **28**, 24-32 (1955).
 - ⁶ Shoenberg, D. *Superconductivity*. Cambridge University Press, 74 (1952).
 - ⁷ Bardeen, J., Cooper, L. N. & Schrieffer, J. R. Theory of superconductivity. *Phys. Rev.* **108**, 1175-1204 (1957).
 - ⁸ Ginzburg, V. L. & Landau, L. D. To the Theory of Superconductivity. *Zh. Eksp. Teor. Fiz.* **20** (12), 1064-1082 (1950).
 - ⁹ Maxwell, E. Isotop Effect in the Superconductivity of Mercury. *Phys. Rev.* **78**, 477-477 (1950).
 - ¹⁰ Reynolds, C. A., Serin, B., Wright, W. H. & Nesbitt, L. B. Superconductivity of Isotopes of Mercury. *Phys. Rev.* **78**, 477-477 (1950).
 - ¹¹ Lasarev, B. & Kan, L. Measurements at low temperatures and high pressures: Superconductivity of Sn and In under uniform compression pressure of 1750 kg/cm². *Zh. Eksp. Teor. Fiz.* **14** (12), 463-473 (1944).
 - ¹² Lorenz, B. & Chu, C. W. High Pressure Effects on Superconductivity. 459-497, in *Frontiers in Superconducting Materials*, Edited by Anant V. Narlikar, Springer Berlin Heidelberg (2005).
 - ¹³ Qin, S., Kim, J., Niu, Q. & Shih, C. K. Superconductivity at the Two-Dimensional Limit. *Science* **324**, 1314-1317 (2009).
 - ¹⁴ N. Kopnin, *Theory of Nonequilibrium Superconductivity*, International Series of Monographs on Physics (2000).
 - ¹⁵ Aranson, I. S. & Kramer, L. The world of the complex Ginzburg-Landau equation. *Rev. Mod. Phys.* **74**, 99-143 (2002).
 - ¹⁶ Note, in particular, the useful Ehrenfest relation $\partial \log T_c / \partial p \simeq \alpha_L / \Delta C_p$, where ΔC_p is the change in the specific heat at the superconductor transition.
 - ¹⁷ Dagotto, E. Complexity in Strongly Correlated Electronic Systems. *Science* **309**, 257-262 (2005).
 - ¹⁸ Ghosal, A., Randeria, M. & Trivedi, N. Role of Spatial Amplitude Fluctuations in Highly Disordered *s*-Wave Superconductors. *Phys. Rev. Lett.* **81**, 3940-3943 (1998).
 - ¹⁹ Ghosal, A., Randeria, M. & Trivedi, N. Inhomogeneous pairing in highly disordered *s*-wave superconductors. *Phys. Rev. B* **65**, 014501 (2001).
 - ²⁰ Dubi, Y., Meir, Y. & Avishai, Y. Nature of the superconductor-insulator transition in disordered superconductors. *Nature* **449**, 876-880 (2007).
 - ²¹ Imry, Y., Strongin, M. & Homes, C. C. An inhomogeneous Josephson phase in thin-film and high- T_c superconductors. *Physica C* **468** 288-293 (2008).
 - ²² Sacépé, B., Chapelier, C., Baturina, T. I., Vinokur, V. M., Baklanov, M. R. & Sanquer, M. Disorder-induced inhomogeneities of the superconducting state close to the superconductor-insulator transition. *Phys. Rev. Lett.* **101**, 157006 (2008).
 - ²³ Fazio, R. & Schön, G. Charge and vortex dynamics in arrays of tunnel junctions. *Phys. Rev. Lett.* **43**, 5307 (1991).
 - ²⁴ Bielejec, E., Ruan, J. & Wu, W. Hard Correlation Gap Observed in Quench-Condensed Ultrathin Beryllium. *Phys. Rev. Lett.* **87**, 036801 (2001).
 - ²⁵ Bielejec, E. & Wu, W. Field-Tuned Superconductor-Insulator Transition with and without Current Bias. *Phys. Rev. Lett.* **88**, 206802 (2002).
 - ²⁶ Sambandamurthy, G., Engel, L.W., Johansson, A. & Shahar, D. Superconductivity-Related Insulating Behavior. *Phys. Rev. Lett.* **92**, 107005 (2004).
 - ²⁷ Sambandamurthy, G., Engel, L.W., Johansson, A., Peled, E. & Shahar, D. Experimental Evidence for a Collective Insulating State in Two-Dimensional Superconductors. *Phys. Rev. Lett.* **94**, 017003 (2005).
 - ²⁸ Baturina, T. I., Strunk, C., Baklanov, M. R. & Satta, A. Quantum Metallicity on the High-Field Side of the Superconductor-Insulator Transition. *Phys. Rev. Lett.* **98**, 127003 (2007).
 - ²⁹ Baturina, T. I., Mironov, A. Yu., Vinokur, V. M., Baklanov, M. R. & Strunk, C. Localized Superconductivity in the Quantum-Critical Region of the Disorder-Driven Superconductor-Insulator Transition in TiN Thin Films. *Phys. Rev. Lett.* **99**, 257003 (2007).
 - ³⁰ Fistul, M. V., Vinokur, V. M. & Baturina, T. I. Collective Cooper-Pair Transport in the Insulating State of Josephson-Junction Arrays. *Phys. Rev. Lett.* **100**, 086805 (2008).
 - ³¹ Vinokur, V. M., Baturina, T. I., Fistul, M. V., Mironov, A. Yu., Baklanov, M. R. & Strunk, C. Superinsulator and quantum synchronization. *Nature* **452**, 613-615 (2008).
 - ³² Pomeau, Y. & Rica, S. Dynamics of a model of supersolid. *Phys. Rev. Lett.* **72**, 2426-2429 (1994).